Heterodimers Based on CoPt 3 −Au Nanocrystals with Tunable Domain Size

ARTICLE *in* JOURNAL OF THE AMERICAN CHEMICAL SOCIETY · JUNE 2006

Impact Factor: 12.11 · DOI: 10.1021/ja0607741 · Source: PubMed

J|A|C|S
ARTICLES
Published on Web 05/02/2006

Heterodimers Based on $CoPt_3$−Au Nanocrystals with Tunable Domain Size

Teresa Pellegrino,*,† Angela Fiore,† Elvio Carlino,‡ Cinzia Giannini,§ P. Davide Cozzoli,† Giuseppe Ciccarella,† Marc Respaud,¶ Luca Palmirotta,† Roberto Cingolani,† and Liberato Manna†

Contribution from the National Nanotechnology Laboratory of CNR-INFM, Distretto Tecnologico ISUFI, 73100 Lecce, Italy, TASC-INFM-CNR National Laboratory, Area Science Park, Basovizza, 34012 Trieste, Italy, CNR-Istituto di Cristallografia (IC), via Amendola 122/O, 70126 Bari, Italy, and LNMO-INSA, 135 avenue de Rangueil, Toulouse, France

Received February 1, 2006; E-mail: teresa.pellegrino@unile.it

Abstract: We describe an approach to synthesize colloidal nanocrystal heterodimers composed of $CoPt_3$ and Au. The growth is based on the nucleation of gold domains on preformed $CoPt_3$ nanocrystals. It is a highly versatile methodology which allows us to tune independently the size of the two domains in each dimer by varying several reaction parameters. The statistical analysis of the distribution of the domain sizes in the dimers and the compositional mapping achieved by dark field imaging and energy dispersive spectroscopy confirm that the two domains in each dimer are indeed made of $CoPt_3$ and Au, respectively. Structural characterization by high-resolution transmission electron microscopy shows that the two domains, both having cubic fcc Bravais lattice, can share a common {111}, {100}, or {110} facet, depending on the size of the initial $CoPt_3$ seeds. The magnetization measurements evidence a ferromagnetic $CoPt_3$ phase with a relatively low anisotropy as a consequence of their disordered crystalline structure, regardless of the presence of a Au tip. We believe that this prototype of nanocrystal dimer, which can be manipulated under air, can find several applications in nanoscience, as the Au section can be exploited as the preferential anchor point for various molecules, while the $CoPt_3$ domain can be used for magnetic detection.

Introduction

Smart nanosystems consisting of various sections, each characterized by peculiar physical properties, surface chemistry, size, and morphology, would be ideal for the development of new bottom-up nanotechnologies.[1−4] Prototype structures exploiting this concept are, for instance, the chemically synthesized colloidal inorganic nanocrystals, in which inorganic domains of different materials are directly assembled in a "hybrid" nanocrystal, with no need of organic molecule bridges.[5−12] One type of hybrid nanocrystal is the core−shell structure,[1,8] in which a nanocrystalline core is covered by a shell of another material. So far, different types of core−shell nanocrystals have been prepared by exploiting various mechanisms. The most studied core−shell nanocrystals are based on two or more types of semiconductors,[13−16] such as the highly fluorescent CdSe@ZnS nanocrystals,[14,15] in which the ZnS shell improves the photoluminescence quantum yield of the CdSe cores. More recent examples include, for instance, Ag@Co core−shells, obtained by the thermolysis of a mixture of Co and Ag organometallic precursors, during which a selective nucleation of silver nanoparticles is followed by the deposition of Co on top of the formed nuclei.[17] With a slightly different mechanism, semiconductor-magnetic core−shells of Co@CdSe have been grown by nonepitaxial deposition of CdSe on the surface of preformed Co nanoparticles.[18] These nanocrystals showed a transition from the superparamagnetic to the ferromagnetic behavior at room temperature, as a consequence of the reduction of the strength

† National Nanotechnology Laboratory of CNR-INFM.
‡ TASC-INFM-CNR National Laboratory.
§ CNR-Istituto di Cristallografia.
¶ LNMO-INSA.

(1) Dawson, A.; Kamat, P. V. *J. Phys. Chem. B* **2001**, *105* (5), 960−966.
(2) O'Neal, D. P.; Hirsch, L. R.; Halas, N. J.; Payne, J. D.; West, J. L. *Cancer Lett.* **2004**, *209* (2), 171−176.
(3) Cozzoli, P. D.; Manna, L. *Nat. Mater.* **2005**, *4* (11), 801−802.
(4) Pellegrino, T.; Kudera, S.; Liedl, T.; Munoz Javier, A.; Manna, L.; Parak, W. J. *Small* **2005**, *1* (1), 48−63.
(5) Lu, Y.; Xiong, H.; Jiang, X. C.; Xia, Y. N.; Prentiss, M.; Whitesides, G. M. *J. Am. Chem. Soc.* **2003**, *125* (42), 12724−12725.
(6) Gu, H. W.; Zheng, R. K.; Zhang, X. X.; Xu, B. *J. Am. Chem. Soc.* **2004**, *126* (18), 5664−5665.
(7) Gu, H. W.; Yang, Z. M.; Gao, J. H.; Chang, C. K.; Xu, B. *J. Am. Chem. Soc.* **2005**, *127* (1), 34−35.
(8) Green, M. *Small* **2005**, *1* (7), 684−686.
(9) Mokari, T.; Rothenberg, E.; Popov, I.; Costi, R.; Banin, U. *Science* **2004**, *304* (5678), 1787−1790.
(10) Milliron, D. J.; Hughes, S. M.; Cui, Y.; Manna, L.; Li, J. B.; Wang, L. W.; Alivisatos, A. P. *Nature* **2004**, *430* (6996), 190−195.
(11) Mokari, T.; Sztrum, C. G.; Salant, A.; Rabani, E.; Banin, U. *Nat. Mater.* **2005**, *4* (11), 855−863.
(12) Kudera, S.; Carbone, L.; Casula, M. F.; Cingolani, R.; Falqui, A.; Snoeck, E.; Parak, W. J.; Manna, L. *Nano Lett.* **2005**, *5* (3), 445−449.
(13) Eychmuller, A.; Mews, A.; Weller, H. *Chem. Phys. Lett.* **1993**, *208* (1−2), 59−62.
(14) Hines, M. A.; Guyotsionnest, P. *J. Phys. Chem.* **1996**, *100* (2), 468−471.
(15) Dabbousi, B. O.; Rodriguez Viejo, J.; Mikulec, F. V.; Heine, J. R.; Mattoussi, H.; Ober, R.; Jensen, K. F.; Bawendi, M. G. *J. Phys. Chem. B* **1997**, *101* (46), 9463−9475.
(16) Peng, X. G.; Schlamp, M. C.; Kadavanich, A. V.; Alivisatos, A. P. *J. Am. Chem. Soc.* **1997**, *119* (30), 7019−7029.
(17) Sobal, N. S.; Hilgendorff, M.; Mohwald, H.; Giersig, M.; Spasova, M.; Radetic, T.; Farle, M. *Nano Lett.* **2002**, *2* (6), 621−624.
(18) Kim, H.; Achermann, M.; Balet, L. P.; Hollingsworth, J. A.; Klimov, V. I. *J. Am. Chem. Soc.* **2005**, *127* (2), 544−546.

10.1021/ja0607741 CCC: $33.50

of the dipolar interactions. The modification of the photoluminescence properties in the core−shell systems as compared to those of pure CdSe particles cannot be unambiguously attributed to the ferromagnetic core. Bimagnetic core−shell nanocrystals have been synthesized by using FePt nanoparticles as seeds for the subsequent growth of Fe_3O_4.[19] By tuning the thickness of the Fe_3O_4 shell, the magnetic properties of the nanoparticles could be varied, as the exchange coupling between the core and the shell materials was modified. Several iron-based magnetic core−shell nanocrystals were reported also by Kauzlarich and co-workers.[20]

Another type of hybrid structure is the heterodimer,[5−8] in which two or more inorganic domains are joined together through a small interfacial area. Heterodimers of submicrometer colloidal particles have been reported in the past few years.[5,21,22] Heterodimers of nanocrystals smaller than 100 nm can be prepared from materials that have large interfacial energy or when only certain regions on the surface of a starting nanocrystal core can be chemically accessed by the other material. Recent examples of such hybrid nanostructures are nanocrystal dimers of CdS−FePt, which have been synthesized by thermal decomposition of sulfur and cadmium precursors in the presence of FePt nanoparticles.[6] Upon annealing, the shell of CdS that initially grows on the FePt nanoparticles coalesces and forms a separate sphere attached at one side to the original FePt nanoparticle. This process is probably driven by the lattice mismatch, by the large interfacial energy, and presumably also by the immiscibility between the two materials. As a further example, Au−Fe_3O_4 nanocrystal dimers have been synthesized by thermolysis of $Fe(CO)_5$, followed by oxidation of Fe, in the presence of gold seeds.[23] The formation of these dimers was presumably due to the difference in lattice constants and to an electron-induced charge polarization at the interface between the two materials when iron oxide nucleated on the gold nanocrystals. The latter effect made the remaining gold facets deficient in electrons, and no additional nucleation occurred on the gold nanocrystals. A recently reported route to obtain iron oxide−silver heterodimers is based on the self-assembly of iron oxide nanoparticles at the liquid−liquid interface of a biphasic system, where the iron oxide nuclei provide catalytic sites for reducing silver ions to metallic silver.[7] This approach was adopted also to form other types of heterodimers, such as FePt−Ag, Au−Ag, and Fe_3O_4−Au.[7]

While significant advance has been made on the preparation of these new types on hybrid materials, an unaddressed issue in the growth of heterodimers is the independent control of the size of the two domains, which would clearly make these nanostructures highly versatile for practical applications. In this paper, we report an approach to fabricate a new type of heterodimer, based on one $CoPt_3$ domain and on one Au domain, for both of which we have achieved such control. The formation of this heterodimer is due to the selective nucleation of a gold on a single facet of a $CoPt_3$ nanocrystal. Heterodimers with tunable geometric parameters can be synthesized through a systematic variation of parameters, such as the size of the initial $CoPt_3$ nanoparticle, the growth temperature, and the concentration of the Au precursors. By using a combination of techniques, we demonstrate that the growth of Au on $CoPt_3$ is highly epitaxial, and that the two domains of the heterostructure are indeed composed of Au on one side and of a low anisotropic ferromagnetic $CoPt_3$ phase on the other side. At higher temperature, the nanoparticles became superparamagnetic. Interestingly, the growth of Au tips does not affect the magnetic properties of $CoPt_3$ nanoparticles.

Experimental Section

Chemicals. Cobalt carbonyl ($Co_2(CO)_8$, stabilized with 1−5% hexane) and platinum(II)−acetylacetonate ($Pt(acac)_2$, 99%) were purchased from Strem. Hexadecylamine (HDA, 90%), 1,2-hexadecanediol (90%), gold(III) chloride ($AuCl_3$, 99%), dodecylethyldimethylammonium bromide (DEDAB, 98%), diphenyl ether (99%), dodecylamine (>99%), and 1,2-dichlorobenzene (99%) were purchased from Sigma-Aldrich. 1-Adamantanecarboxylic acid (ACA, >99%) was purchased from Fluka. Unless otherwise stated, all syntheses were carried out under air-free conditions, using the standard Schlenk line setup.

Synthesis of $CoPt_3$. $CoPt_3$ nanocrystals with sizes ranging from 3 to 10.5 nm were prepared following a literature procedure,[24,25] with minor changes. As an example, in a typical synthesis of monodisperse $CoPt_3$ with an average diameter of 9 nm, 0.033 g of $Pt(acac)_2$, 4 g of HDA, 0.25 g of ACA, 0.13 g of 1,2-hexadecanediol, and 2 mL of diphenyl ether were mixed in a 50 mL three-neck flask, heated to 65 °C, and degassed for 20−30 min. The reaction mixture was heated to 200 °C under vigorous stirring, and the cobalt stock solution (0.014 g of $Co_2(CO)_8$ dissolved in 0.7 mL of 1,2-dichlorobenzene) was injected into it. The solution was kept at 200 °C for 60 min and then was heated at 290 °C for an additional 45 min. To isolate the nanocrystals, 2-propanol was added to the flask before the mixture solidified, and the precipitate was redispersed in toluene, under air. The nanocrystals were precipitated again to wash out the excess of stabilizers.

The concentration of the $CoPt_3$ nanocrystal solution was determined by gravimetric measurements. $CoPt_3$ nanocrystals were precipitated from a clean solution in toluene (by addition of 2-propanol) and were dried under nitrogen. From the average nanocrystal diameter, as measured by TEM, and from the density of bulk $CoPt_3$ (which is 18.86 g/cm^3), the average mass of a single nanoparticle was calculated. The number of nanoparticles in the original toluene solution (and so their concentration) was estimated by dividing the total mass of the dried precipitate by the estimated average mass of a single nanoparticle. For example, for a $CoPt_3$ nanoparticle of 7 nm, we have calculated a mass equal to 3.38×10^{-15} mg. This procedure, however, tends to overestimate the number of particles, as the mass of the surfactant molecules that coat the nanocrystal surface is not taken into account.

Synthesis of the $CoPt_3$−Au Dimers. Dimers of $CoPt_3$−Au were prepared by nucleation of Au on preformed $CoPt_3$ nanoparticles. As a general procedure, a solution of $AuCl_3$, DEDAB (which forms a soluble complex with $AuCl_3$), and dodecylamine in toluene was added dropwise to a colloidal solution of $CoPt_3$ nanoparticles kept under inert atmosphere. In all the experiments, the molar ratio between $AuCl_3$ and dodecylamine was equal to 1:8, and the ratio between $AuCl_3$ and DEDAB was equal to 1:1.8. In a typical synthesis, 6.5 mL of a 6 μM solution of $CoPt_3$ nanocrystals in toluene (corresponding, therefore, to 3.9×10^{-2} μmol of nanocrystals) was diluted by the addition of 50 mL of toluene. The resulting solution was heated to 60 °C under vigorous stirring and under N_2 flow. The gold stock solution was

(19) Zeng, H.; Li, J.; Wang, Z. L.; Liu, J. P.; Sun, S. H. *Nano Lett.* **2004**, *4* (1), 187−190.
(20) Cho, S. J.; Idrobo, J. C.; Olamit, J.; Liu, K.; Browning, N. D.; Kauzlarich, S. M. *Chem. Mater.* **2005**, *17* (12), 3181−3186.
(21) Yin, Y. D.; Lu, Y.; Xia, Y. N. *J. Am. Chem. Soc.* **2001**, *123* (4), 771−772.
(22) Yin, Y. D.; Lu, Y.; Gates, B.; Xia, Y. N. *J. Am. Chem. Soc.* **2001**, *123* (36), 8718−8729.
(23) Yu, H.; Chen, M.; Rice, P. M.; Wang, S. X.; White, R. L.; Sun, S. H. *Nano Lett.* **2005**, *5* (2), 379−382.
(24) Shevchenko, E. V.; Talapin, D. V.; Rogach, A. L.; Kornowski, A.; Haase, M.; Weller, H. *J. Am. Chem. Soc.* **2002**, *124* (38), 11480−11485.
(25) Shevchenko, E. V.; Talapin, D. V.; Schnablegger, H.; Kornowski, A.; Festin, O.; Svedlindh, P.; Haase, M.; Weller, H. *J. Am. Chem. Soc.* **2003**, *125* (30), 9090−9101.

prepared by dissolving 115 mg of $AuCl_3$ (0.38 mmol), 223 mg of DEDAB (0.69 mmol), and 592 mg of dodecylamine (3.19 mmol) in 25 mL of toluene, followed by sonication for 20 min at room temperature, during which the color of the solution changed from dark orange to light yellow. This stock solution was added dropwise to the reaction mixture over a total time of 60 min, after which the flask was kept at 60 °C for an additional 3 h and then under overnight stirring at room temperature. The appearance of Au surface plasmon absorption, which indicated gold nucleation, occurred after an induction period of 5−10 h, depending on the size of the starting $CoPt_3$ seeds, on the $CoPt_3$:Au molar ratio, and on the temperature. Subsequent growth of the gold domains in the heterodimers was not accompanied by further absorption changes. From TEM analysis, an increase in the heterodimer fraction at progressively longer reaction times was observed. After the synthesis, methanol was added to the reaction mixture, and the solution was centrifuged at 2000 rpm for 10 min. The supernatant, which contained unreacted $AuCl_3$ and unbound surfactants, was discarded, and the precipitate was redissolved in toluene.

Power X-ray Diffraction (XRD). XRD measurements were performed with a Rigaku diffractometer equipped with a rotating anode source, a Ge(111) single-crystal monochromator, and a curved position sensitive INEL detector collecting 120° at once. Concentrated nanocrystal solutions were spread on top of a silicon substrate, then the sample was allowed to dry, and measured in reflection geometry.

Transmission Electron Microscopy (TEM). Low-magnification TEM images were recorded on a JEOL Jem 1011 microscope operated at an accelerating voltage of 100 kV. TEM samples were prepared by dropping a dilute solution of nanocrystals in toluene on carbon-coated copper grids (Formvar/Carbon 300 Mesh Cu) and by letting the solvent evaporate. In all the syntheses of $CoPt_3$ nanocrystals and of the corresponding heterodimers, a statistical analysis was carried out on several wide-field, low-magnification TEM images, by counting at least 300 nanoparticles. On the bare $CoPt_3$ nanocrystals, the average nanocrystal diameter was determined. On the dimers, their average length was determined. This was defined as the length of the dimer along the common axis of the two domains. Samples composed of dimers in which the two domains had similar sizes were called "symmetric". Samples composed of dimers in which one domain was significantly larger than the other were called "asymmetric". In this latter case, from the average length of the dimers, it was possible to extract the average diameter of the larger and of the smaller domain, respectively. This determination clearly had no meaning for less asymmetric or almost symmetric dimers.

Phase contrast high-resolution transmission electron microscopy (HRTEM), high angle annular dark field (HAADF) scanning transmission electron microscopy (STEM), and energy-dispersive X-ray spectroscopy (EDS) experiments were performed to understand the structural and chemical nature of the heterodimers. The experiments were performed by using a JEOL 2010F TEM/STEM microscope equipped by Oxford EDS spectrometer and YAP large-angle detector for HAADF imaging. The microscope was operated at 200 keV, corresponding to an electron wavelength of 0.00251 nm. The objective lens has a spherical aberration coefficient of 0.47 ± 0.01 nm and, hence, a resolution at optimum defocus in HRTEM of 0.19[26] and of 0.126 nm in HAADF imaging.[27] The chemical composition of individual $CoPt_3$ nanocrystals and of dimers was examined through a combination of HAADF imaging in STEM and EDS mapping, acquired by scanning an electron probe with a diameter of 0.1 nm within the clusters. For the EDS maps, an acquisition time of 6000 s was used. During data acquisition, the specimen drift correction was active, checking for possible drift every 60 s. After 6000 s, a total correction of the order of 4 nm had been gradually implemented.

(26) Spence, J. *Experimental High-Resolution Electron Microscopy*; Oxford: New York, 1988; p 87.
(27) Carlino, E.; Grillo, V. *Proceedings of the 7th Multinational Congress on Microscopy: MCM 2005*; Portoroz, Slovenia, June 26−30, 2005; p 6303.

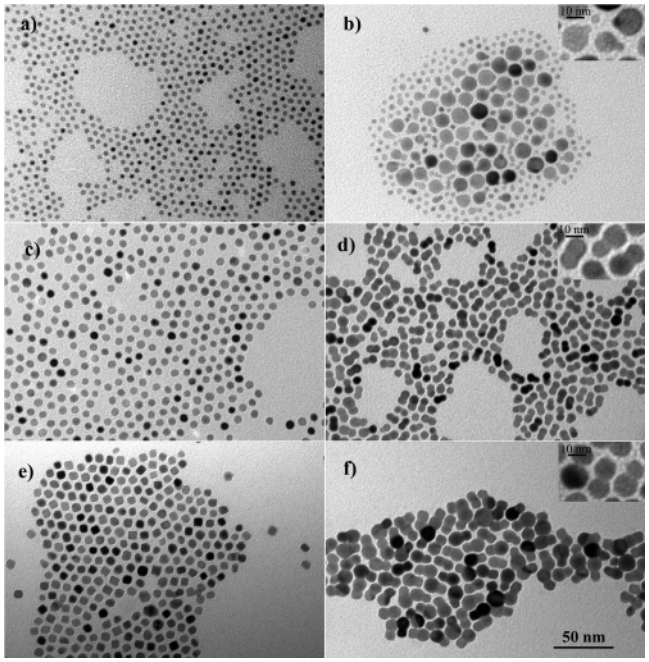

Figure 1. Heterodimers prepared from $CoPt_3$ nanocrystals of different sizes. (a), (c), and (e) are the TEM images of the initial $CoPt_3$ nanoparticles, and (b), (d), and (f) are the images of the corresponding dimers. The scale bar for all images is as the one shown in (f), except for the insets, for which a scale bar of 10 nm is always reported. Starting from 4.0 nm (a), 6.4 nm (c), and 8.8 nm (e) $CoPt_3$ nanoparticles, dimers were prepared which had average lengths corresponding to 11.9 nm (b), 12.5 nm (d), and 15.7 nm (f), respectively. The smallest $CoPt_3$ nanoparticles led to the most asymmetric dimers. In this case, the average size of the smaller domains in the dimers corresponded to that of the original $CoPt_3$ nanocrystals. Therefore, the larger domains in the dimer should be Au nanoparticles (see the inset of b). The dimers obtained from 6.4 and 8.8 nm $CoPt_3$ nanoparticles were more symmetric in shape (see insets of d and f for a higher magnification view of a few dimers). The estimated percentages of heterodimers referred to the samples of pictures b, d, and f are 40, 80, and 90%, respectively.

Compositional Analysis on Nanocrystal Ensembles. Inductively coupled plasma atomic emission spectrometer Varian Vista AX was used to investigate the elemental composition of the nanocrystals. Samples were dissolved in HCl/HNO_3 3:1 (v/v) by using a CEM "MARS 5" microwave digester.

Magnetic SQUID Measurements. Magnetization measurements were performed in order to investigate the influence of the growth of Au tips on $CoPt_3$ on the magnetic properties. They were performed on a SQUID magnetometer (MPMS Quantum Design). The temperature was varied between 2 and 400 K according to a classical zero-field cooling/field cooling (ZFC/FC) procedure in the presence of a very weak applied magnetic field (10 Oe), and the hysteresis cycles were obtained at different temperatures in a magnetic field varying from +50 to −50 kOe. The samples were prepared in gelatin capsules under air.

Results

Effect of the Size of the Initial $CoPt_3$ Nanoparticles. In a series of experiments, $CoPt_3$ nanocrystals with average sizes corresponding to 4.0 ± 0.5, 6.4 ± 0.7, and 8.8 ± 1.0 nm were prepared. Starting from these particles, heterodimers were synthesized with average lengths equal to 11.9 ± 2.4, 12.5 ± 1.7, and 15.7 ± 2.4 nm, respectively. Low-resolution TEM images of the starting nanocrystals and of the resulting heterodimers are shown in Figure 1. In all the syntheses, the concentration of the $CoPt_3$ solution was kept constant (1.84 μM), while the amount of Au(III) precursors injected was scaled up

in order to find the best conditions to grow the dimers. Therefore, for each synthesis of heterodimers, we will report the ratio between the moles of $AuCl_3$ injected and the moles of $CoPt_3$ nanoparticles present in the flask (henceforth referred to as "Au:$CoPt_3$ ratio" for brevity).

The formation of dimers starting from the sample containing small $CoPt_3$ nanocrystals (4.0 nm in diameter, Figure 1a) was a rather difficult process and, in fact, only a few dimers were observed, whereas most of the original $CoPt_3$ nanocrystals appeared to have not reacted at all (Figure 1b). The few heterodimers formed were strongly asymmetric, with the smaller sphere having a radius comparable to that of the original $CoPt_3$ nanoparticles, from which it could be preliminarily inferred that the larger domains in this sample were made of Au. In this synthesis, the Au:$CoPt_3$ ratio was 7.3×10^3. At lower ratios (i.e., when less $AuCl_3$ was injected), even fewer dimers were formed, which were largely asymmetric, as well. At higher ratios (more $AuCl_3$ injected), only remarkably large Au nanoparticles were observed (with diameters exceeding 200−300 nm), and it was not possible to distinguish whether each of these particles had a small nanocrystal (the original $CoPt_3$ nanocrystal) attached to it. When trying to grow Au on even smaller $CoPt_3$ nanocrystals (3 nm in diameter; see Figure S1 of the Supporting Information, SI), again only very large Au particles were found in the final sample, regardless of the Au:$CoPt_3$ ratio used. Also, in this case, it was not possible to identify any small nanoparticle attached to such large nanocrystals.

More symmetric dimers could be grown when starting from bigger $CoPt_3$ nanocrystals (6.4 and 8.8 nm in diameter), as can be seen in Figure 1c−f. In the syntheses that yielded the samples shown in Figure 1d and 1f, the Au:$CoPt_3$ ratio was equal to 6.2×10^3 and to 9.7×10^3, respectively (see Table 1 of SI for more details on the experimental conditions and Table 4 for the statistics on the size).

Effect of the Au:$CoPt_3$ Ratio. In general, for a sample of $CoPt_3$ nanocrystals of a given average diameter, the size of the Au domain in the corresponding dimer was dependent on the Au:$CoPt_3$ ratio used. As an example, we report here three heterodimers prepared from the same sample of $CoPt_3$ nanocrystals (8.8 nm in diameter) but grown at different Au:$CoPt_3$ ratios, namely, 4.0×10^3, 1.0×10^4, and 1.7×10^5 (Figure 2b, c, and d, respectively; see also Table 2 of the SI for more details). Gold domains were able to nucleate on such large particles even at Au:$CoPt_3$ ratios as low as 4.0×10^3. In this case, the gold domains were smaller on average than the starting $CoPt_3$ nanocrystals (Figure 2b). Heterodimers with more symmetric shapes were observed when the Au:$CoPt_3$ ratio was increased to 1.0×10^4 (Figure 2c), as the gold had grown on average to a size comparable to that of the starting $CoPt_3$ nanoparticles. Interestingly, these symmetric structures were always accessible over a wide range of Au:$CoPt_3$ ratios. For instance, roughly symmetric dimers were still observed at a ratio as high as 5×10^4, although in these cases, also aggregates of big Au nanoparticles were present and were separated by the rest of the sample by centrifugation. When the Au:$CoPt_3$ ratio was raised further to 1.7×10^5, the dimers were again asymmetric, but the gold domains were bigger on average than the starting $CoPt_3$ nanoparticles (Figure 2d) (see also Table 4 of the SI for the statistics on size). Also, a considerable amount of aggregates of large gold nanocrystals was collected after centrifugation.

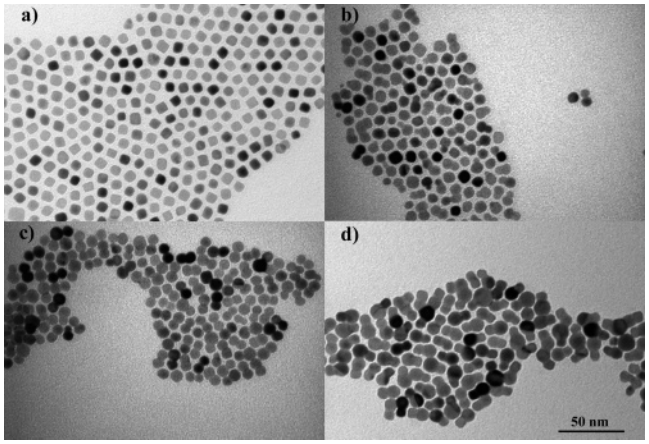

Figure 2. Heterodimers grown starting from the same sample of $CoPt_3$ nanocrystals (8.8 nm in diameter) (a) but at different Au:$CoPt_3$ ratios: (b) 4.0×10^3; (c) 1.0×10^4; and (d) 1.7×10^5. The concentration of $CoPt_3$ nanocrystals was the same in all these syntheses. The estimated percentages of heterodimers referred to the samples of pictures b, c, and d are 40, 90, and 70%, respectively.

Effect of the Temperature. The growth of heterodimers was carried out at 60 °C, as described previously. However, the effect of different growth temperatures was also studied. As an example, we report the results of three syntheses carried out on the same batch of $CoPt_3$ nanocrystals (8.3 nm in diameter). In this series of experiments, all the reaction conditions were the same, except for the reaction temperature, which was set at 25, 60, and 90 °C, respectively. In general, higher temperatures led to higher yields of dimers and in addition promoted the formation of larger Au domains in the dimers. Some dimers could be seen already in the synthesis carried out at 25 °C, although their yield was remarkably low (see Figure 3a). At 60 °C, the yield of dimers was much higher (about 80%), and in addition, they were more symmetric in shape (Figure 3b). Finally, in the synthesis carried out at 90 °C, the dimers were more asymmetric, with the smaller domain being comparable in size to the starting $CoPt_3$ nanocrystals (Figure 3c) (see also Tables 3 and 6 of the SI).

Structural Characterization by TEM/STEM. HRTEM analysis gave a detailed picture of the structure of the heterodimers. Figure 4 shows, for instance, HRTEM images of typical heterodimers, often surrounded by $CoPt_3$ nanocrystals. In all the dimers, no lattice fringe distortion has been observed at the interface between the two domains, indicating good lattice match. This is somehow a surprising result because there should be a lattice mismatch of 4% between Au and $CoPt_3$. In principle, for perfect epitaxial growth, only a few monolayers of Au should be able to grow on $CoPt_3$ before plastic relaxation occurs. In the dimers shown in Figure 4, both domains have a face centered cubic (fcc) Bravais lattice. Analysis of these images reveals that the facet shared by the two domains in the dimer corresponds to the {100} facet (Figure 4a), the {111} facet (Figure 4b), and the {110} facet (Figure 4c) of the fcc lattice, respectively. In particular, we found that the {111} facet is the most frequently shared one in asymmetric dimers obtained from small $CoPt_3$ nanocrystals (4−6 nm in diameter). In addition, Figure 4a and 4b shows that, in some cases, additional nanocrystals start adding to the original dimers. This was sometimes observed in solution when large concentrations of starting $CoPt_3$ nanocrystals were employed or when the mixture was left to react well beyond

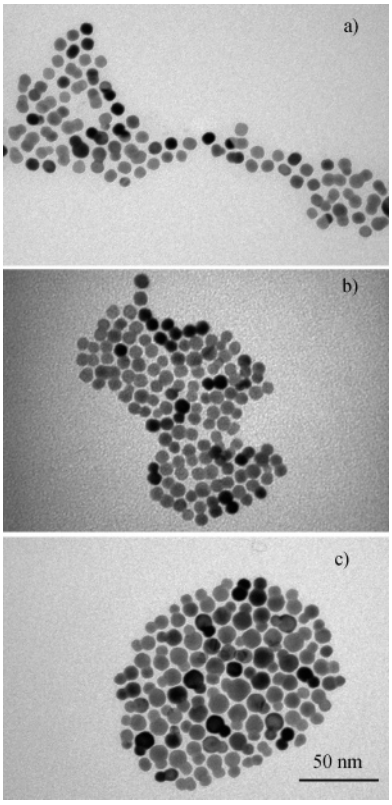

Figure 3. Heterodimers grown from the same sample of $CoPt_3$ nanocrystals (8.3 nm in diameter) and at the same Au:$CoPt_3$ ratio, but at different temperatures: (a) 25 °C; (b) 60 °C; and (c) 90 °C. The estimated percentages of heterodimers referred to the samples of pictures a, b, and c are 20, 80, and 90%, respectively.

the time required to form dimers. Occasionally, the attachment of nanocrystals to a preformed dimer was also observed to occur in situ in the TEM over several hours, when a dimer was closely surrounded by nanocrystals[28] (Figure 4b actually represents the earliest stage of this in situ attachment event, as the nanocrystals on the bottom left and on the bottom of the dimer are starting to attach to the dimer).

To elucidate the compositional nature of the nanocrystals, detailed in situ analyses were carried out. Panels a and b of Figure 5, for instance, are representative high angle annular dark field (HAADF) images with over-imposed relevant energy-dispersive X-ray spectroscopy (EDS) map obtained by scanning 0.1 nm electron probe and by acquiring the characteristic X-ray photons for Pt $L\alpha1$ (shown in red) and Au $L\alpha1$ (shown in green). The EDS maps show the row counts as acquired, without taking into account the relevant cross sections and without any background subtraction. Despite the long acquisition time, the counts in the map are relatively few (about 2000 counts for Au and 200 counts for Pt, for instance, for Figure 5a) due to the very small size of the electron probe and the thinness of the sampled region. Such a small probe size is required in order to obtain the necessary spatial resolution. In addition, the number of characteristic Au and Pt X-ray photons counted is low because for more than 50% of the acquisition time the beam was scanned in the region around the particles, where mostly the carbon film was sampled. Nevertheless, such spatially resolved analysis allowed us to identify the two particles in the dimer as made mainly of Au (the bigger particle) and Pt (the smaller particle). The map of the isolated "small" particles (such as the one on the lower left side of Figure 5a) shows on the other hand mainly Pt $L\alpha1$ counts, along with a few Au $L\alpha1$ counts. The presence of a few Pt $L\alpha1$ counts in the region dominated by Au $L\alpha1$ counts (the big domain) and of a few Au $L\alpha1$ counts in the domain richer in Pt $L\alpha1$ counts could be due either to an intermixing of Pt and Au or simply to the background, as at this level of statistics the Pt counts are of the order of the background counts. It is worthwhile to remark that both EDS and HAADF experiments cannot distinguish between an actual intermixing and a surface adhesion among different chemical species. With this respect, however, it seems unlikely that Au−Pt intermixing occurs at the temperature at which the dimers are formed (60−90 °C).

Complementary information on the composition of the nanocrystals could be obtained by HAADF imaging. Indeed, the intensity in the HAADF image is strongly related to the mean atomic number of the specimen and to its thickness. Figure 5c is a HAADF image of a group of nanocrystals, including dimers and isolated nanoparticles. Clusters with the same size but higher HAADF image intensity have a content of chemical species with relatively higher atomic number. Hence, most of the small clusters are made of $CoPt_3$, whereas three of them, visible in the central group of particles, have a higher atomic number and are, very likely, made of Au. Hence, most of the small particles are $CoPt_3$, although some of them appear to be made of Au. In the asymmetric dimers, the larger domain appears brighter, an effect that can be interpreted as both arising from composition and thickness. On the other hand, even on isolated nanocrystals that appear to be $CoPt_3$ (based on their overall intensity in low-magnification HAADF), atomic resolution *Z*-contrast observations show the presence of some Au atoms. Figure 5d, for instance, shows a HAADF image at atomic resolution of an isolated $CoPt_3$ nanocrystal which did not develop into a dimer. In the image, brighter spots indicate the presence of Au contamination in the cluster (most likely on its surface). Therefore, traces of Au are likely to be present on all the $CoPt_3$ nanocrystals, also on those on which have not developed into dimers.

Powder XRD Spectra. Figure 6 reports the powder XRD spectra of a sample of $CoPt_3$ nanocrystals and of a sample of dimers grown from these particles. The diffraction pattern of the $CoPt_3$ particles could be ascribed to the disordered fcc phase, as already observed for this type of material.[24,25] The lattice unit cell parameter ($a = 3.8889$ Å) is slightly larger than the one reported in the literature for the disordered fcc phase of $CoPt_3$ (3.853 Å).[29] The elemental analysis revealed that the Co:Pt ratio was 1:2.95, very close to the 1:3 ratio which corresponds to the $CoPt_3$ alloy. The X-ray diffraction spectrum of the heterodimers shows the typical diffraction patterns of nanosized Au and $CoPt_3$ particles. The Au crystalline phase is fcc, as well (unit cell $a = 4.0803$ Å, space group $fm3m$). All peak positions and widths related to $CoPt_3$ remain practically unchanged after Au growth, indicating that the Au growth process does not modify the size nor the composition of the starting $CoPt_3$ nanocrystals.

(28) Jose-Yacaman, M.; Gutierrez-Wing, C.; Miki, M.; Yang, D. Q.; Piyakis, K. N.; Sacher, E. *J. Phys. Chem. B* **2005**, *109* (19), 9703−9711.

(29) Pearson, W. B. *A Handbook of Lattice Spacings and Structures of Metals and Alloys*; Pergamon: Oxford, 1964.

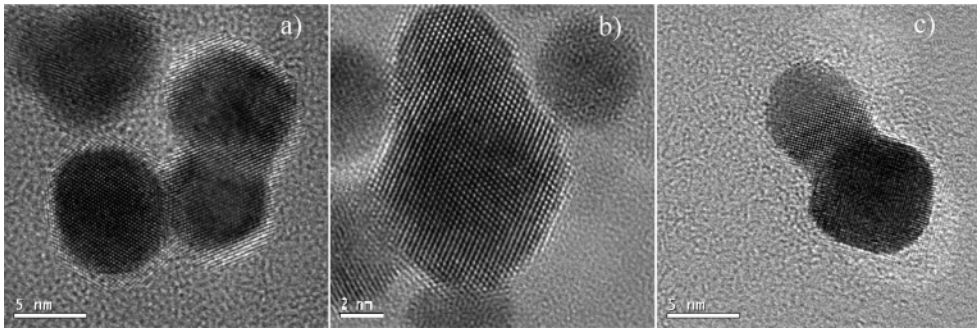

Figure 4. Phase contrast, high-resolution TEM image of dimers showing epitaxy and sharing a {200} plane (a), a {111} plane (b), and a {220} plane (c), respectively.

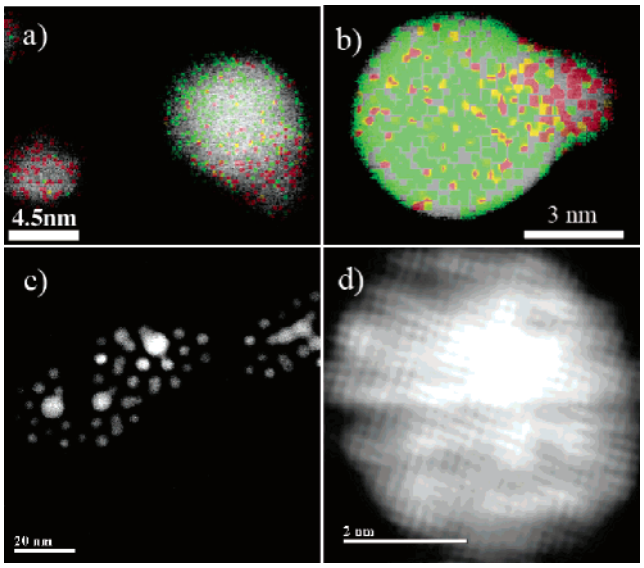

Figure 5. Energy-dispersive X-ray spectroscopy (EDS) map of an isolated nanocrystal (a, bottom-left side) and of two dimers (a, right side, and b) obtained by scanning a 0.1 nm electron probe and by acquiring the characteristic X-ray photons for Pt $L\alpha 1$ (shown in red) and Au $L\alpha 1$ (shown in green). (c) Low-magnification HAADF image of a group of nanocrystals, including various dimers and isolated nanoparticles. (d) High-magnification HAADF image of an isolated $CoPt_3$ nanoparticle, showing the presence of Au contamination on the nanocrystal.

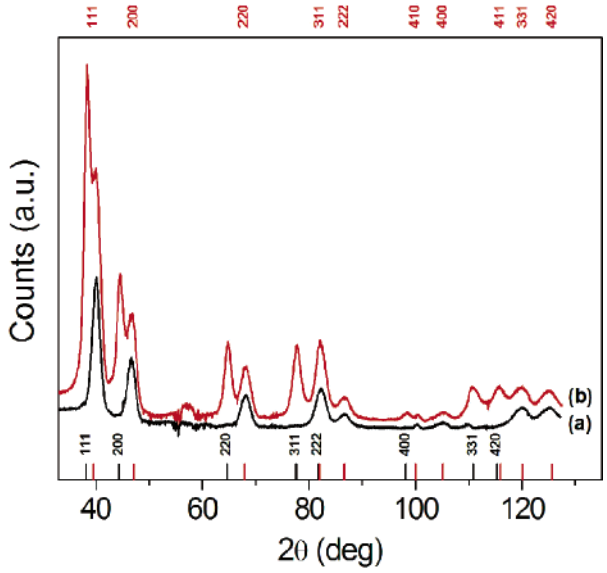

Figure 6. Powder XRD spectra of a sample of $CoPt_3$ nanocrystals (black line) and of a sample of dimers grown from the same $CoPt_3$ particles (red line).

Magnetic Measurements. These were done on $CoPt_3$ nanocrystals with an average diameter of 8.6 ± 1.4 nm and on the dimers derived from these particles. Figure 7a displays the hysteresis loops measured at a temperature of 2 K on the $CoPt_3$ nanocrystals and on the corresponding heterodimers having 15.7 ± 2.4 nm in length. All the magnetization measurements have been systematically normalized with respect to the saturated magnetization of each system. Both curves are characteristic of ferromagnetic nanoparticles in the blocked state. The remnant magnetization is half of the saturation magnetization, as expected in the case of uniaxial anisotropic nanoparticles. The coercive fields are nearly the same, 70 and 73 mT, for the $CoPt_3$ nanocrystals and for the heterodimers, respectively. The magnetization curve measured after a field cooling from 400 K in a magnetic field of 5 T does not evidence any shift of the hysteresis loops. This latter feature enables us to conclude that no thick Co oxide layer has grown on the nanocrystals, even if these had been exposed to air. The low-field magnetization measured in a low field of 1 mT, according to the zero-field cooled−field cooled (ZFC−FC) procedure, evidences a superparamagnetic transition above the blocking temperature of 68 K for the $CoPt_3$ nanocrystals (see Figure 7b). It falls down to 50 K in the case of the dimers. The measurement of the magnetization at 5 T as a function of the temperature shows a gradual decrease of the spontaneous magnetization, leading to a Curie temperature just above 400 K in the two cases. The low coercive fields measured at low temperature (lower than 0.1 T) and the Curie temperature are typical of $CoPt_3$ nanoparticles crystallized according to the disordered fcc phase.[30−33]

Discussion

The mechanism by which dimers are formed is based on the heterogeneous nucleation of gold on the surface of the $CoPt_3$ nanocrystals. The reducing agent is the dodecylamine, and the $CoPt_3$ nanocrystals act as nucleation sites (or as catalysts) for the redox reaction. We support this mechanism by several experimental evidences and by performing a series of control experiments. First, if no dodecylamine was present in the Au

(30) Sanchez, J. M.; Moran-Lopez, J. L.; Leroux, C.; Cadeville, M. C. *J. Phys.: Condens. Matter* **1989**, *1*, 491−496.
(31) Wiekhorst, F.; Shevchenko, E.; Weller, H.; Kotzler, J. *Phys. Rev. B* **2003**, *67* (22).
(32) O'Connor, C. J.; Sims, J. A.; Kumbhar, A.; Kolesnichenko, V. L.; Zhou, W. L.; Wiemann, J. A. *J. Magn. Magn. Mater.* **2001**, *226−230*, 1915−1917.
(33) Ely, T. O.; Pan, C.; Amiens, C.; Chaudret, B.; Dassenoy, F.; Lecante, P.; Casanove, M. J.; Mosset, A.; Respaud, M.; Broto, J. M. *J. Phys. Chem. B* **2000**, *104* (4), 695−702.

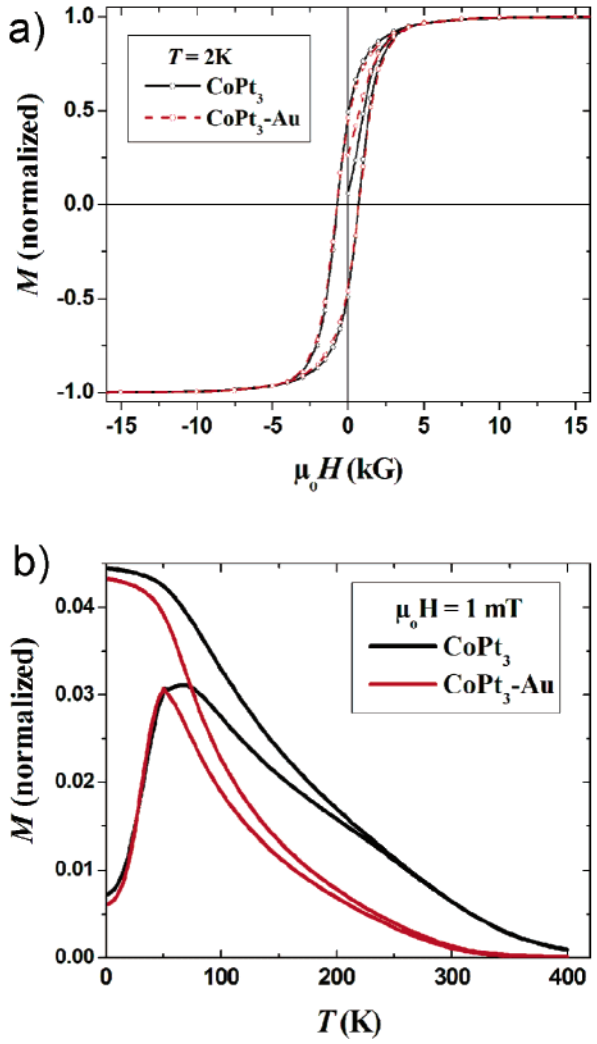

Figure 7. (a) Hysteresis loops measured at a temperature of 2 K for both the monomers and heterodimers. The $CoPt_3$ cores have a diameter of 8.6 nm. The magnetization curves have been normalized with respect to the saturation magnetization. (b) Zero-field cooled/field cooled magnetizations measured at a magnetic field of 1 mT for the same samples as in (a).

stock solution, neither dimers nor isolated gold nanocrystals were formed, proving that the amine is the reducing agent, whereas the $CoPt_3$ nanocrystals basically remain unchanged in the sole presence of $AuCl_3$. Furthermore, $CoPt_3$ nanocrystals are necessary for the redox reaction to occur between Au(III) and the amine. If the gold stock solution was injected in bare toluene at 60 °C, with no $CoPt_3$ nanoparticles present, and all the conditions were followed as described above for the standard synthesis of heterodimers, no formation of Au nanocrystals occurred. The observed growth of gold on top of $CoPt_3$ has thus a close analogy to several reported nanocrystal syntheses in which a seed-catalyzed redox process triggers the growth of larger spherical[34] or rod-like metal nanoparticles[35−39] or yet metallic core−shell systems.[40,41] To our knowledge, however, this is the first example of heterodimer formation by means of a seeded growth mechanism. Indeed, the role of dodecylamine as reducing agent in the present system is the same as that of ascorbic acid in the seeded growth of metal nanocrystals.[34−38] Both reducing agents cannot, in fact, accomplish a sufficiently fast reduction of the Au(III) to Au(0) in the absence of metal seeds, although they are able to convert Au(III) into Au(I).[34−39,42] From the perspective of nucleation theory,[43] an equivalent way of understanding this mechanism of growth is that the barrier for the homogeneous nucleation of isolated Au nanocrystals in solution is relatively high, whereas the barrier for heterogeneous nucleation of Au on pre-existing nuclei is much smaller.

We have explored the parameters involved in the formation of Au−$CoPt_3$ heterodimers. There are mainly three: the size of the starting $CoPt_3$ nanocrystals, the Au:$CoPt_3$ ratio, and the reaction temperature. They can be varied independently, yielding a large range of shapes for the dimers. From these experimental data, the seeded growth (or, in other words, the heterogeneous nucleation) mechanism is always supported, as indeed in all the syntheses in which asymmetric dimers were formed, the average diameter of one of the two domains (either the smaller or the larger one, depending on the synthesis conditions) always corresponded, within the statistical error, to the average size of the starting $CoPt_3$ nanocrystals. This is an indication that dimers were formed by nucleation and growth of Au on the existing $CoPt_3$ nanocrystals, whose size did not change during this process.

On the basis of the evidence discussed so far, we exclude that the formation of dimers is due to the nucleation of isolated Au nanocrystals, followed by their attachment to the existing $CoPt_3$ nanocrystals. Although oriented attachment is indeed one of the most effective pathways to anisotropic nanostructures,[44−48] and coalescence of metal nanoparticles is also a well-known effect,[28] any sort of fusion mechanism would imply in our case that Au nanocrystals should nucleate first in solution, and as such, they should be able to do so even in the absence of $CoPt_3$ nanocrystals. Nucleation of Au nanocrystals in the absence of $CoPt_3$, as reported above, has not been observed in control experiments. As a further control experiment, heating a toluene solution in which preformed Au nanocrystals (coated with tetraoctylammonium bromide) and $CoPt_3$ nanoparticles had been mixed did not lead to the formation of dimers. In addition, in the hypothesis of a fusion mechanism, there is no apparent reason why only two particles should attach to each other, and therefore, also aggregates of several particles should form. In our samples, we could see only isolated nanocrystals and a very large population of dimers over other types of aggregates, and this discredits the fusion among isolated particles as the mechanism of formation of heterodimers. Finally, compositional

(34) Jana, N. R.; Gearheart, L.; Murphy, C. J. *Langmuir* **2001**, *17* (22), 6782−6786.
(35) Jana, N. R.; Gearheart, L.; Murphy, C. J. *Adv. Mater.* **2001**, *13* (18), 1389−1393.
(36) Jana, N. R.; Gearheart, L.; Murphy, C. J. *J. Phys. Chem. B* **2001**, *105* (19), 4065−4067.
(37) Gou, L. F.; Murphy, C. J. *Chem. Mater.* **2005**, *17* (14), 3668−3672.
(38) Nikoobakht, B.; El-Sayed, M. A. *Chem. Mater.* **2003**, *15* (10), 1957−1962.
(39) Perez-Juste, J.; Rodriguez-Gonzalez, B.; Mulvaney, P.; Liz-Marzan, L. M. *Adv. Funct. Mater.* **2005**, *15* (7), 1065−1071.
(40) Henglein, A. *Langmuir* **2001**, *17* (8), 2329−2333.
(41) Srnova-Sloufova, I.; Vlckova, B.; Bastl, Z.; Hasslett, T. L. *Langmuir* **2004**, *20* (8), 3407−3415.
(42) Gomez, S.; Philippot, K.; Colliere, V.; Chaudret, B.; Senocq, F.; Lecante, P. *Chem. Commun.* **2000**, *19*, 1945−1946.
(43) Markov, I. V. *Crystal Growth for Beginners: Fundamentals of Nucleation, Crystal Growth, and Epitaxy*; World Scientific: Singapore, 2003.
(44) Penn, R. L.; Banfield, J. F. *Am. Miner.* **1998**, *83*, 1077−1082.
(45) Weller, H. *Philos. Trans. R. Soc. London Ser. A: Math. Phys. Eng. Sci.* **2003**, *361* (1803), 229−239.
(46) Cho, K. S.; Talapin, D. V.; Gaschler, W.; Murray, C. B. *J. Am. Chem. Soc.* **2005**, *127* (19), 7140−7147.
(47) Ribeiro, C.; Lee, E. J. H.; Longo, E.; Leite, E. R. *ChemPhysChem* **2005**, *6*, 690−696.
(48) Yu, J. H.; Joo, J.; Park, H. M.; Baik, S. I.; Kim, Y. W.; Kim, S. C.; Hyeon, T. *J. Am. Chem. Soc.* **2005**, *127* (15), 5662−5670.

analysis by EDS of several dimers always showed that one domain is richer in Au and the other domain is richer in Pt. We never found dimers in which the two domains had similar composition. If attachment between particles had occurred by fusion, we would expect, for instance, to find also Au−Au or $CoPt_3$−$CoPt_3$ dimers. The occasional presence of isolated Au nanocrystals (see Figure 5c) can be explained by the fact that Au might have nucleated also on very small $CoPt_3$ nanocrystals, so small that they are not clearly visible under TEM. The attachment of nanocrystals to dimers (as shown in Figure 4), and in several cases also the coalescence between two or more dimers, was always observed well after the formation of the dimers. This can be rationalized by considering that the Au domain on each dimer is poorly passivated, and this makes it easily accessible to other species present in solution, including unreacted $CoPt_3$ nanocrystals as well as the Au domains of other dimers. Nevertheless, this coalescence deserves further investigation and will be the subject of a future work.

Our experiments show that on small $CoPt_3$ nanocrystals, with sizes of 3−4 nm, the heterogeneous nucleation of Au is difficult and occurs only on a few nanocrystals. It is likely, in fact, that small nanocrystals cannot offer a sufficiently extended facet for the Au nucleation to occur on it, or perhaps their surface is better passivated than that of larger nanocrystals and, therefore, is less accessible and/or catalytically active. Small $CoPt_3$ nanocrystals always promoted the formation of asymmetric dimers carrying large Au domains. This can be explained by considering that the nucleation of Au only on a few nanocrystals left large amounts of unreacted Au precursors in solution. Therefore, the few Au domains that had nucleated could grow to large sizes due to the large availability of Au monomers in solution via self-catalyzed Au(III) reduction. On bigger $CoPt_3$ nanocrystals (with average sizes ranging from 5 to 10.5 nm), the nucleation of Au domains was much easier, and therefore a higher percentage of dimers was formed. In these cases, the Au domains in the dimers grew to comparatively smaller sizes, as they had to compete more with each other for the monomers left in solution. The dimers in such cases were more symmetric. Similarly, the effect of the temperature on the formation of the dimers can be explained easily. Higher temperatures make the Au precursor more reactive, and therefore more dimers can form and, in addition, the Au domains can grow to larger sizes.

The key point in this work is that Au is not covering uniformly the $CoPt_3$ nanocrystals, but instead it grows only on one facet of the original nanocrystal. Apparently, no additional "patches" of Au form on other facets of the starting nanocrystals. This is in contrast to previous findings on core−shell $CoPt_x$/Au and $FePt_x$/Au nanocrystals, which were reported some years ago[32] (in that case, however, the nanocrystals were synthesized in reverse micelles, at room temperature, and in addition, no TEM images were supplied in the work). We believe that, as soon as Au nucleates on one facet of $CoPt_3$ nanocrystals, it is much easier for additional Au(III) ions from the solution to be reduced on this facet. In other words, the formed Au patch could act as a catalyst[34−39] for the subsequent reduction of additional Au(III), as already hypothesized in the synthesis of Ag-based heterodimers.[7] The one-sided growth of gold on $CoPt_3$ should not be similar to the recently reported one-sided growth of Au on CdSe nanorods,[11] in which Au patches initially grew on both ends of the rods, as these were the only chemically accessible facets. Subsequently, a ripening process occurred via oxidation of the smaller domain and further reduction of Au ions on the larger domain, sustained by charge migration along the rod. At last, the two gold domains transformed into a single, large domain located only on one side of the rod.[11] This mechanism would be possible in our case only if the transient formation of multiple Au domains on a single $CoPt_3$ nanoparticle was observed. However, we never found and isolated these intermediate species in our samples. Also, our experimental data allow us to exclude a dewetting process in the formation of dimers.[5,6] According to this mechanism, a thin shell initially grows uniformly around the particle and then coalesces into a single domain, often upon an annealing process. In the specific case of this work, this process would be driven by the presumably high interfacial energy between Au and $CoPt_3$ and also by the high mobility of Au atoms. After dewetting, the Au domain would be very likely localized on the facet that minimizes the interfacial energy. However, we did not observe the transient formation of such a shell, but the direct formation of dimer structures.

A remarkable point is that the growth of Au on small $CoPt_3$ nanocrystals appears to privilege the {111} type of facet. It is likely that the {111} facets of $CoPt_3$, which have the highest growth rate[25] and therefore the highest chemical reactivity, could be the only accessible facets at small seed size, while others, such as the {100} or the {110} facets, could be better passivated or simply less reactive, or not even well developed. On $CoPt_3$ nanocrystals with larger size, on the other hand, the differences in chemical reactivity among the various facets seem less pronounced, and therefore Au shows no preference on which facet to grow. This fact actually accounts also for the higher dimer yield that was achieved in this case. Overall, the observed dependence of dimer growth on the size of the starting $CoPt_3$ particles agrees well with previous findings,[36,37] highlighting that in seed-catalyzed metal syntheses the characteristics of the seed (such as its size, the presence of surface defects, and the nature of the bound surfactant) ultimately dictate the structure of the resulting nanoparticles.

As for what concerns the magnetic properties of the dimers, the most remarkable result is that the growth of a Au domain on the $CoPt_3$ core does not alter the low-temperature hysteresis loop of the original nanocrystals significantly, which means that the anisotropy field is unaffected by the presence of Au tips. The decrease of the blocking temperature and changes in the shape of the ZFC/FC curves deserve more refined measurements and analysis. However, as in the case of core−shell Co−CdSe nanocrystals,[18] these effects may be connected to the decrease of the magnetic volume fraction with the presence of the Au domain, which induces a reduction of the dipolar interactions between the particles.

Conclusions

In this work, we have reported a simple method to synthesize $CoPt_3$−Au heterodimers based on the heterogeneous nucleation of gold on $CoPt_3$ nanocrystals. This method allows one to tune the sizes of both the gold and the $CoPt_3$ domains by varying parameters, such as the size of the initial $CoPt_3$ nanocrystals, the ratio Au:$CoPt_3$, and the reaction temperature. The formation of dimers involves a seed-catalyzed mechanism, and the growth of Au occurs epitaxially on different facets of starting $CoPt_3$

seeds, depending on their size. Compositional mapping, as well as X-ray diffraction, indicates that the two domains in each dimer are indeed made of Au and $CoPt_3$. In addition, magnetic measurements show that the growth of Au on the original nanocrystals does not modify their magnetic properties significantly. The control of the size of the ferromagnetic particle should allow one to tune the superparamagnetic transition, that is, their relaxation time. These types of heterodimers are likely to find applications in nanoscience, as in each dimer the ferromagnetic $CoPt_3$ domain can be used for magnetic detection in biosensors and/or for directing the dimer under a magnetic field in a specific location of a given environment, while at the same time the Au domain can serve as an anchoring point for various molecules/biomolecules. Furthermore, an envisaged field of application could be, for instance, data storage, as the gold region could prove useful for anchoring the dimers in specific locations and with given orientations on purposely patterned surfaces, yielding ordered arrays of magnetic nanoparticles tightly bound to a substrate. In this case, most of the particles will have the same orientation, therefore yielding a thin film of nanoparticles with a textured magnetic anisotropy.

Acknowledgment. This work was supported in part by the European projects SA-NANO (Contract No. STRP 013698) and OLLA (Contract No. IST 004607). We acknowledge Dr. Bruno Chaudret (LCC-CNRS, Toulouse) and Dr. Katerina Soulantica (LNMO-INSA, Toulouse) for the SQUID measurements. We are also thankful to Roberto Lassandro and Giuseppe Chita (CNR-IC, Bari) for help on the diffraction measurements.

Supporting Information Available: Detailed conditions for the preparation of all the heterodimers reported in this work; results on the statistical analysis on the sizes of the $CoPt_3$ nanocrystals and of the heterodimers; a typical optical absorption spectrum of a sample of $CoPt_3$−Au dimers. This material is available free of charge via the Internet at http://pubs.acs.org.

JA0607741